Electronic Supplementary Information

Strong Reinforcement Effects in 2D Cellulose Nanofibril-Graphene Oxide (CNF-GO) Nanocomposites due to GO-Induced CNF Ordering

Hanieh Mianehrow [a], Giada Lo Re[ab], Federico Carosio[c], Alberto Fina[c], Per Tomas Larsson[ad] , Pan Chen[ae] and Lars A Berglund[a]*

[a] Department of Fibre and Polymer Technology, Wallenberg Wood Science Center, KTH Royal Institute of Technology, Teknikringen 56, 100 44 Stockholm, Sweden

[b] Department of Industrial and Materials Science, Chalmers University of Technology, Rännvägen 2, 412 96 Gothenburg, Sweden

[c] Dipartimento di Scienza Applicata e Tecnologia, Politecnico di Torino, Alessandria Campus, Via Teresa Michel 5, 15121 Alessandria, Italy

[d] RISE Bioeconomy, Drottning Kristinas Väg 61, SE-11486 Stockholm, Sweden

[e] Beijing Engineering Research Center of Cellulose and its Derivatives, School of Materials Science and Engineering, Beijing Institute of Technology, 5 South Zhongguancun Street, Haidian District, Beijing 100081, China

*E-mail: blund@kth.se (LA. B.)

EXPERIMENTAL SECTION

Materials

The never-dried bleached softwood pulp fibers (provided by Nordic Paper Seffle AB, Säffle, Sweden with 14 wt% hemicellulose and < 1% lignin) were subjected to TEMPO-oxidation according to the procedure explained by Saito et al. [1].Sodium bromide (1mmol/g dry pulp) and TEMPO (0.1 mmol/g dry pulp) were added to the pulp suspension (2 wt%). Then sodium hypochlorite (NaClO) (10mmol/gr dry pulp) was added and the pH of the suspension was maintained at the value of 10. The oxidized pulp fibers passed through a high pressure microfluidizer (Microfluidizer M-110EH, Microfluidics Corp, Newton, Massachusetts, USA) to make TEMPO-CNF colloid. A transparent gel was achieved after a single pass through the large chamber (200 μm) and two passes through the smaller chamber (100 μm). The total charge of the oxidized pulp fibers was determined by conductometric titration (SCAN-CM 65) and found to be 1600 μeq g^{-1}. To remove any aggregated fibrils, the as-prepared CNF was diluted by deionized water to make a 0.1wt% suspension of CNF. Then it was dispersed in water using an ultra-turrax at 12,000 RPM for 15 min and then centrifuged at 20,000 RPM and 80% of the supernatant was used for nanopaper preparation. Expandable graphite flakes (grade: 3772) with average lateral size of 300 μm were provided by Asbury Carbons (US), potassium permanganate, nitric acid 67%, sulfuric acid 98% and hydrochloridric acid 37% were purchased from Fisher Scientific (Sweden). Hydrogen peroxide solution 30% was purchased from sigma Aldrich and all materials were used as received.

Synthesis of GO

Large GO sheets were synthesized from natural graphite according to the method used by Aboutalebi et al [2] via preoxidation/thermal expansion of graphite followed by modified Hummer's method [3]. In the first step, 10 g of natural graphite flakes were mixed with 3:1 volume ratio of H_2SO_4:HNO_3 for 24 hours. Then 400 ml of water was added to the resultant solution to stop the reaction. The resultant product was then filtered and washed out with water and left in the oven at 60 ^{0}C for 24 hours. Then, the oxidized graphite was expanded by being introduced to 1000 ^{0}C for 10 seconds in a furnace. In the second step, 1 g of expanded graphite was mixed with 200 ml of H_2SO_4 and 10 g potassium permanganate and left to react for 2 hours. Then 200 ml of distilled water was added to the paste, and the reaction was terminated by addition of 50 ml aqueous solution of H_2O_2 resulting in a yellowish mixture. Then the mixture was centrifuged and washed out three times with 10% HCl solution and then with deionized water at 20,000 rpm until the pH of the solution became around 5-6. As previously described [5] , it is important to start with large graphite flakes and avoid sonication in the preparation process, in order to successfully prepare large GO sheets. Therefore, we started with the largest available graphite flakes (300μm) and did not use sonication. The as-prepared GO suspension was used without any further size fractionation. Information regarding the characterization of synthetized GO is reportedin this file.

Preparation of CNF-GO nanopapers

To make CNF-GO nanopapers with 0.1, 0.5, 1, 2, 4 wt% of GO, different amounts of as-prepared GO dispersion were added to CNF suspension, mixed for 15 minutes and then filtered through vacuum assisted filtration set up using an ultrafiltration membrane (Hydrophilic Polyvinylidene Fluoride (PVDF) (Merck-Millipore), 0.65 μm pore size, 90mm diameter) followed by 15 minutes drying in Rapid Kothen (Rapid-Köthen-RK3A-KWT, PTI laboratory Equipment, Vorchdorf, Austria), sheet former at 90^o C (Figure 1). We wanted comparable thicknesses with similar systems reported in previous literature, where they made 10 micrometer thick films[3, 4]. During the work, we discovered that slightly higher thickness reduced data scatter, so we selected 14 micrometer thickness. No retention agent was used for film formation.

GO weight fraction was converted to volume fraction (ϕ_{GO}) by using the following equation:

$$\phi_{GO} = \frac{w_{GO}}{w_{GO} + \left(\frac{\rho_{GO}}{\rho_{CNF}}\right)(1 - w_{GO})}$$

where w_{GO} is the weight fraction of GO in the composite, ρ_{GO} is the density of GO which is considered (2.2 g/cm^3) [2] and ρ_{CNF} is the density of CNF (1.46 g/cm3) [4].

Characterization techniques

AFM: Atomic force microscopy images were captured with a multimode Nanoscope IIIa Atomic Force Microscope (AFM) produced by Bruker Corp. The AFM was operated in the Scan Assist mode, and RTESP7 cantilevers having a nominal tip radius of 8 nm and a spring constant of 40 N/m (Bruker Corp.) were used. Prior to the test, a piece of silicon wafer was rinsed with ethanol and water and was plasma treated for 2 min, then it was immersed in 1wt% PVA solution for 5 min and after raising with water and drying it was immersed with GO dispersion (0.01 g/L) for 5 min and left to dry after rinsing with water.

TEM: Transmission electron microscope was done using Hitachi HT-7700, Japan operated at 80 kV. A very dilute sample of GO dispersion (0.01 g/L) was deposited on a carboncoated copper grid (Ultrathin Carbon Film/Holey Carbon, Ted Pella). Then, the sample was stained with a droplet of uranyl acetate (2 wt % in deionized water) and left to dry.

Raman: Raman spectra in the range 1000-3200 cm^{-1} were collected on a Renishaw micro-Raman spectrometer equipped with a 532 nm laser (50x magnification, 50mW).

UV-VIS: Ultra violet-visible spectra of GO suspension was collected by a UV-2550 Shimadzu spectrophotometer from 200-600 nm with 1nm interval.

FTIR-ATR: Fourier transformed-infrared spectra in attenuated total reflectance were collected at room temperature in the range 4000-700 cm^{-1} (16 scans and 4 cm-1 resolution) using a spectrometer (Perkin Elmer mod. Frontier) equipped with a diamond crystal.

TGA: Thermogravimetric analyses of prepared GO were performed on a TGA- Discovery TA Instruments under nitrogen or synthetic air atmosphere. The sample (approx. 0.45 mg) was placed in open platinum pans and heated from 50 to 800°C using a heating rate of 10°C/min.

Zeta Potential: The Zetasizer ZEN3600 instrument from Malvern Instruments Ltd., U.K. was utilized for charge determination of CNF, GO and CNF-GO suspensions with the concentration of (0.01 g/L).

Colloidal suspension rheology:

The viscoelastic behavior of the water suspensions was analyzed by a dynamic oscillatory rheometer in a controlled strain rheometer (DHR-2 rheometer, TA Instruments) equipped with a geometry 25 mm parallel plate, Peltier plate Steel - 105050. The water content of all the samples was kept constant (0.7 wt% of solid in 99.3 wt% water), for the sake of a fair comparison. CNF or CNF/GO gels were directly loaded and between the plates and rheological tests were carried out at 25 °C with a gap distance of 2 mm under nitrogen atmosphere. Before each measurement, the samples were allowed to rest for 3-5 min. Covers around samples and silicon oil were used to avoid the sample drying. Oscillatory amplitude strain sweep tests were performed from the initial strain value of

10^{-2} to a final strain value of 100 %, with the frequency of 1 Hz at 25 °C, to determine the linear viscoelastic region of the samples. In frequency sweep test, a small oscillatory amplitude strain, $\gamma = \gamma_0 \sin(\omega t)$ was applied to the samples, by using an amplitude strain value in the linear viscoelastic region (γ_0 = 0.1 %).
The shear stress was expressed as:

$$\sigma(t) = \gamma_0 [G'(\omega)\sin(\omega t) + G'' \cos(\omega t)]$$

Storage shear modulus (G') and complex viscosity (η*) were measured as a function of angular frequency (ω), varying the frequency (f) in the range of 0.001–100 Hz.

Optical transmittance: To measure the transmittance a very high brightness light source whose spectrum spans from UV near-IR wavelengths (170−2100 nm; EQ-99 from Energetiq technology Inc.) was used. The incident beam was first directed into an integrating sphere through one port. Light was directed out of another port of the sphere through an optical fiber, which was recorded by a spectrometer as the WHITE (W) spectrum of the incidence. DARK (D) spectrum was then recorded by turning off the light source. The sample was then put just in front of the sphere's input port, and SIGNAL (S) spectrum was then measured. The transmittance spectrum was then (S − D)/(W − D).

Tensile testing: Rectangular CNF-GO nanopapers with the dimension of 6×50×0.014 mm were tested by a Instron 5944 single column, Universal Testing Machine, equipped with a video extensometer, at a deformation rate of 10%/min. The samples were conditioned at 50% relative humidity and 23° C for two days prior to tensile test. The modulus was recalculated using the data collected by the video extensometer at 0.2-0.5 % strain.

Stress relaxation: The relaxation of stress in CNF-GO nanopaper was investigated by subjecting them to a step strain of 0.1% and measuring stress relaxation behavior of nanopaper by 5944, 2KN Instron tensile tester for 300 sec.

FESEM: Scanning electron microscopy (SEM) images were captured by Hitachi S-4800, Hitachi Corp., Japan equipped with a field emission electron gun. The following settings were used: 5 kV in acceleration voltage, a probe current of 5 μA, and a working distance of 8.5 mm. All samples were sputtered for 30 second with platinum-palladium.

In-plane Synchrotron measurements: the small angle X-ray scattering (SAXS) and wide angle X-ray scattering (WAXS) measurements were carried out at LiX beamline (ID16) of the National synchrotron light source INSLS-II at brookhaven national labororary, New York, US. Three dectectors allow to collect data with the scattering vector ranging from 3 to 0.005 A^{-1}. For each sample, twenty individual 1s second exposures were performed and two incident direactions (in-plane and cross-plane) were measured.

SAXS measurement: Small Angle X-ray Scattering (SAXS) measurement were performed on a point collimated Anton Paar SAXSpoint 2.0 system (Anton Paar, Graz, Austria) equipped with a Microsource X-ray source (Cu K□ radiation, wavelength 0.15418 nm) and a Dectris 2D CMOS Eiger R 1M detector with 75 micrometres by 75 micrometres pixel size.

All measurements were performed with a beam size of approximately 500 micrometers diameter, at a sample stage temperature between 25 °C to 29 °C (no temperature control was employed) with a beam path pressure at about 1-2 mbar. The sample to detector distance (SDD) was 575.7 mm.

All samples were mounted on a Sampler for solids (Anton Paar, Graz, Austria) mounted on a VarioStage (Anton Paar, Graz, Austria). The samples were exposed to vacuum during measurement. For each sample 6 frames each of 10 minutes duration were

read from the detector, giving a total measurement time of 1 hour per sample. For all samples the relative transmission and thickness were determined and used for scaling of the scattering intensities.

The software used for instrument control was SAXSdrive version 2.01.224 (Anton Paar, Graz, Austria), and post-acquisition data processing was performed using the software SAXSanalysis version 3.00.042 (Anton Paar, Graz, Austria).

SAXS Analysis: The in-plane orientation of CNFs with and without GO was calculated from azimuthal profile of 200 reflections using following equations:

Degree of Orientation (Π) = $\frac{180 - FWHM}{180}$ (FWHM= full width at half maximum)

Hermans orientation factor (f) = $\frac{3 < cos^2\varphi > \ - 1}{2}$ (φ = azimuthal angle)

$$< cos^2\varphi > \ = \frac{\int_0^{\pi/2} I(\varphi)\, cos^2\varphi \sin\varphi \, d\varphi}{\int_0^{\pi/2} I(\varphi) \sin\varphi \, d\varphi}$$

Oxygen permeability: Oxygen permeability measurements in humid condition (90 % R.H.) were assessed using an Extraperm apparatus (Extra solutions, Italy). Due to the small size of the prepared GO-based films, sample have been tested using an aluminum mask to reduce the exposed area to 2.01 cm^2. The experimental error was found to be within ±5 %.

Supplementary Figures and Tables

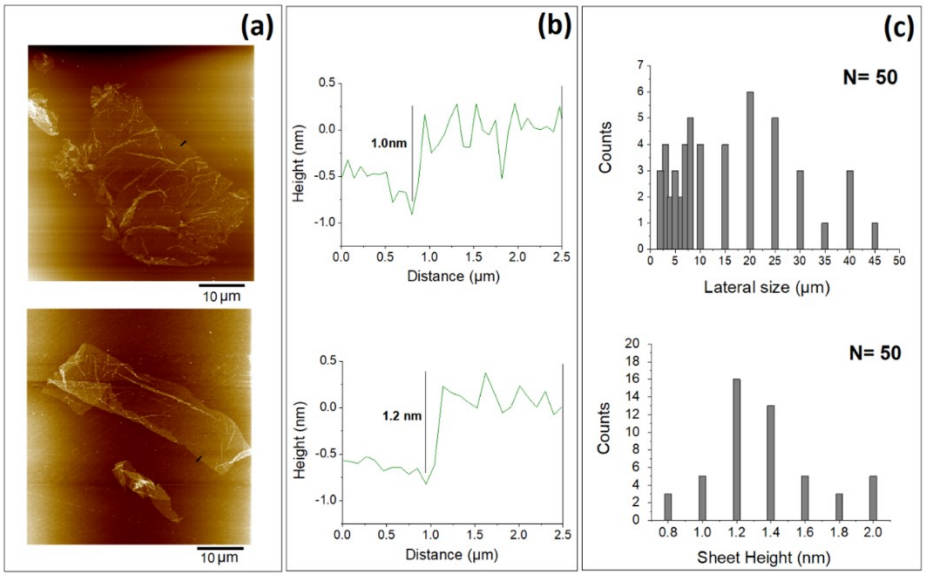

Figure S1: AFM images of as-prepared GO (a) with corresponding height profiles (b) size and height distribution of synthesized GO sheets (c)

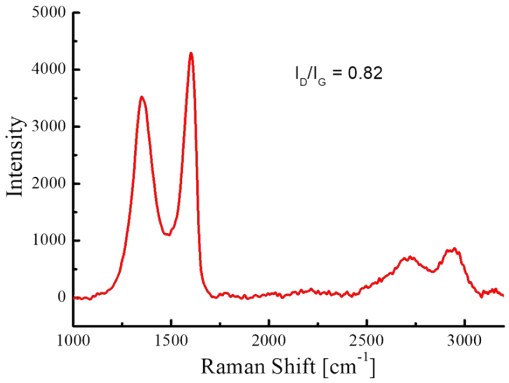

Figure S2: Raman spectrum of prepared GO

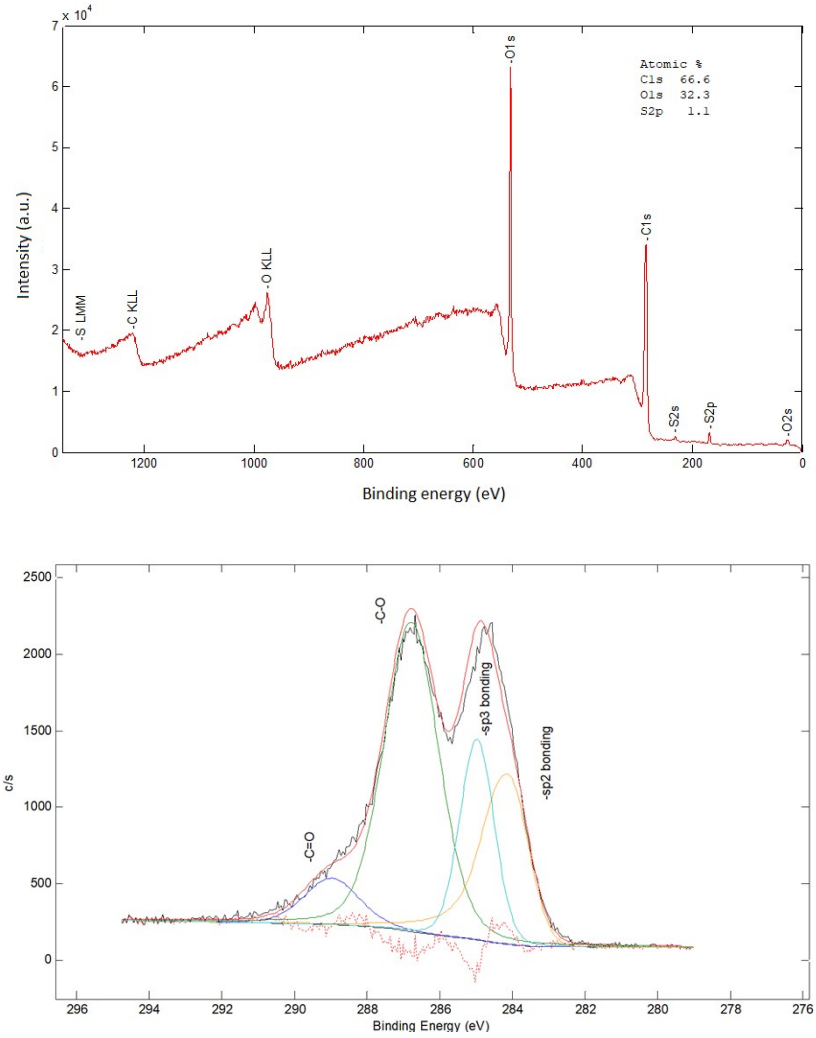

Figure S3: XPS analysis of prepared GO

IR spectroscopy data for GO (Figure S4 and Table S1) show the presence of oxidized functionalities (namely COOH, C=O and C-OH) resulting from the GO preparation process [5]. The thermal stability of the GO was evaluated by TGA in nitrogen and in air atmosphere (Figure S4). In both atmospheres the first weight loss (≈ 7% up to 150°C) is associated with water removal. In the 150-300°C range, this is followed by the release of CO, CO_2 and water from the most labile functional groups (weight loss ≈ 40%) [6]. Above 300°C the remaining residue is further converted into a more ordered graphite-like structure in nitrogen (final residue 37 %, at 800 °C). For the case of air environment, the GO is completely oxidized (final residue 0%).

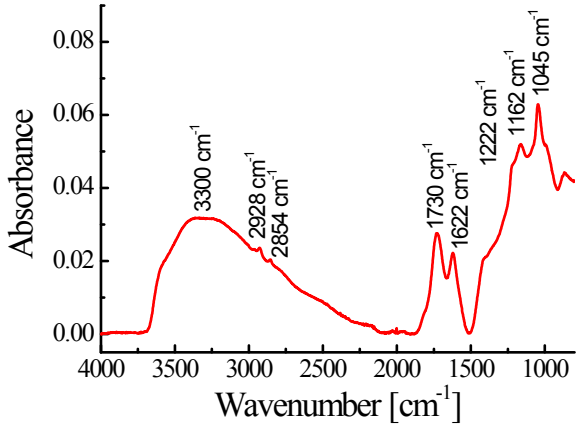

Figure S4: ATR spectrum of prepared GO

Table S1: IR peaks of prepared GO

Wavenumber [cm^{-1}]	**Functional group**
2400 - 3600 band	-OH str. Adsorbed H_2O
2928	C-H asym. str.
2854	C-H sym. str.
1730	C=O str. (broad peak suggest overlapping of different groups, including carboxyl, ketones or aldehydes)
1622	Adsorbed H_2O
1407 (sh.)	S=O asym. str.
1222 (sh.)	S=O sym. str.

1164	C-H bend.
1045	C-H bend. C-O str.

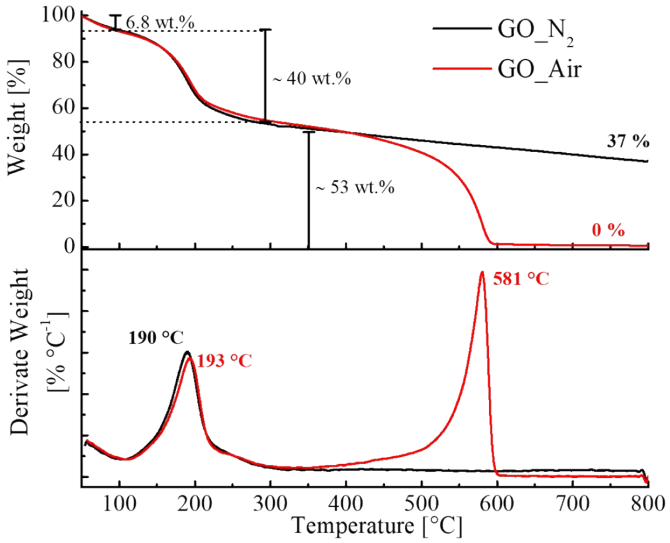

Figure S5: Thermogravimetric analysis in nitrogen and air atmosphere of prepared GO

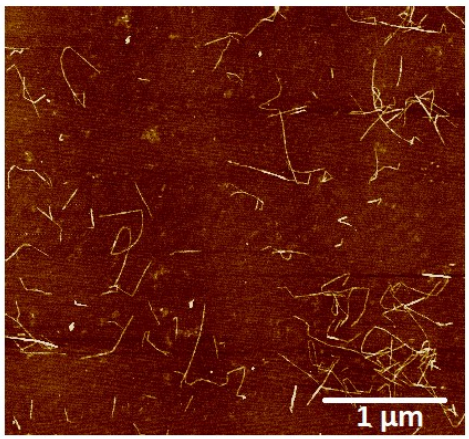

Figure S6: AFM image of TEMPO-CNF with diameter of 2-4 nm and lengths of 0.2-1 µm

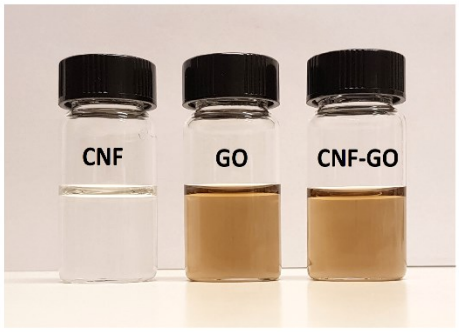

Figure S7: Photograph of CNF, GO and CNF-GO suspensions.

CNF and GO suspensions show zeta potential values of -50.8 ± 5.6 mV (CNF) and -42 ± 2.0 mV (GO), and the zeta potential of a mixed suspension of CNF and GO (50:50) was -36.8 ± 3.00 mV. Zeta potential values higher than ±30 mV are often considered as a criterion for a stable suspension [96]. The favorable colloidal stability of CNF-GO suspensions is a prerequisite in order to prepare films of well-dispersed GO platelets in CNF matrix.

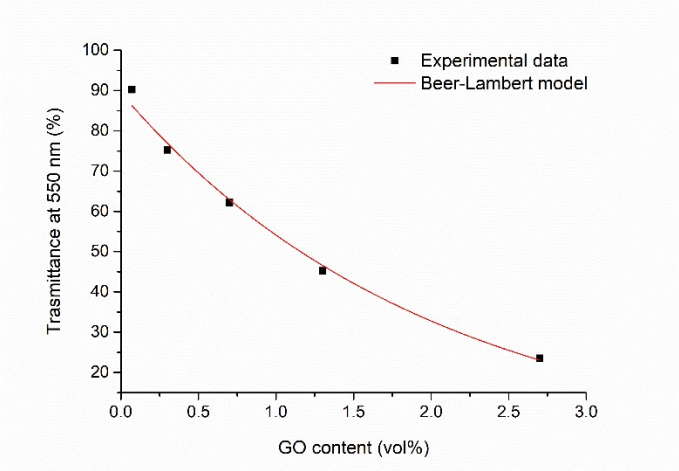

Figure S8: Experimental data for optical transmittance (T) at 550 nm versus GO content, and fit to Beer-Lambert model using (ε) = 160 cm^{-1} (R^2 = 0.99).

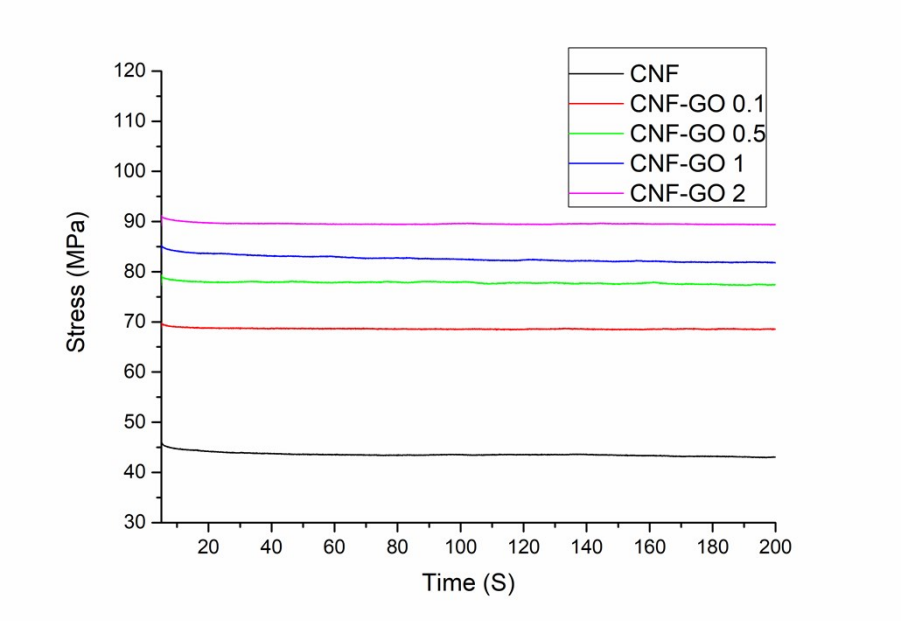

Figure S9: Stress relaxation curves for neat CNF and CNF-GO nanopapers at different wt% of GO

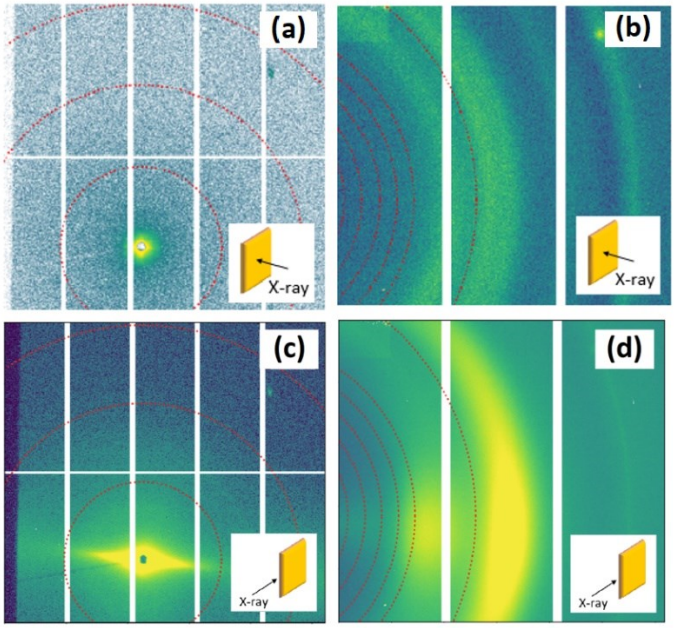

Figure S10. SAXS and WAXS diffraction patterns of CNF-GO 0.07 measured when X-ray beam is perpendicular (a and b) and parallel (c and d) to the film's plane

Some additional information is provided for the data in Table 2:

Xu et al [11] made films based on banana petiole CNF and GO with GO contents up to 8.45 wt%. They improved tensile strength, better thermal stability and higher storage modulus for the composites. However, the modulus improvement was not very high.

They reached a Young's modulus of 4.8 GPa at 8.45 wt% GO as compared with 3.8 GPa for neat CNF film. The reason for the low modulus of the neat CNF film is unclear. Beeran et al [12] made nanocomposites based on two types of CNFs : non-oxidized and TEMPO-oxidized, in combination with ammonia-functionalized GO (NGO). They used 0.5-3 wt% NGO and reported enhancement in dielectric performance of the composites. The maximum Young's modulus was 3.4 GPa and ultimate strength was 88.3 MPa for TEMPO-CNF based composite with 3 wt% GO. The Young's modulus and ultimate strength of neat TEMPO-CNF were 2.04 GPa and 74.5 MPa respectively. Song et al [18] made nanocomposites based on CNF and graphene sheets (10 wt%) as flexible heat spreaders. They investigated the effect of graphene sheet defects on thermal and mechanical properties of the nanocomposites and obtained the best results with low defect graphene sheets (nanocomposite data: E= 6.2 GPa, ultimate strength 117 MPa). Li et al [21] made nacre-like nanocomposite films based on polydopamine (PDA)-modified CNF and graphene. They reported improved thermal conductivity for the modified nanocomposites compared with non-modified nanocomposites at 10 wt% graphene. Enhancement in tensile strength was described, but no Young's modulus values were reported. Duan et al [13] made nacre-like nanocomposites based on CNF, GO/RGO and 10,12-pentacosadiyn-1-ol (PCDO) as crosslinker. They used high filler contents (up to 97 wt%). A tensile strength of 315 MPa and toughness of 9.8 MJ/m^3 (area under stress-strain curve) was reported for composites at 95 wt% rGO. Young's modulus was not reported. Yang et al [17] made nanocomposite based on CNF and graphene (10-90 wt%) and applied mechanical compression to improve alignment of graphene sheets. They reported a slight increase in the Young's modulus of the nanocomposites up to 7.4 GPa (at 30 wt% graphene) compared with 6 GPa for neat CNF. Tensile strength and strain to failure were reduced. The present study differs from those in Table 2 in that the reinforcement content is substantially lower, yet the mechanical properties are very high.

References:

1. T. Saito, M. Hirota, N. Tamura, S. Kimura, H. Fukuzumi, L. Heux and A. Isogai, *Biomacromolecules*, 2009, **10**, 1992-1996.
2. S. H. Aboutalebi, M. M. Gudarzi, Q. B. Zheng and J. K. Kim, *Advanced Functional Materials*, 2011, **21**, 2978-2988.
3. W. S. Hummers Jr and R. E. Offeman, *Journal of the american chemical society*, 1958, **80**, 1339-1339.
4. C. C. Sun, *International journal of pharmaceutics*, 2008, **346**, 93-101.
5. A. M. Dimiev and S. Eigler, *Graphene oxide: fundamentals and applications*, John Wiley & Sons, 2016.
6. P. Cui, J. Lee, E. Hwang and H. Lee, *Chemical Communications*, 2011, **47**, 12370-12372.
7. P. Laaksonen, A. Walther, J. M. Malho, M. Kainlauri, O. Ikkala and M. B. Linder, *Angewandte Chemie International Edition*, 2011, **50**, 8688-8691.
8. N. D. Luong, N. Pahimanolis, U. Hippi, J. T. Korhonen, J. Ruokolainen, L.-S. Johansson, J.-D. Nam and J. Seppälä, *Journal of Materials Chemistry*, 2011, **21**, 13991-13998.
9. J.-M. Malho, P. i. Laaksonen, A. Walther, O. Ikkala and M. B. Linder, *Biomacromolecules*, 2012, **13**, 1093-1099.
10. K. Gao, Z. Shao, X. Wu, X. Wang, J. Li, Y. Zhang, W. Wang and F. Wang, *Carbohydrate polymers*, 2013, **97**, 243-251.
11. C. Xu, G. Wang, C. Xing, L. M. Matuana and H. Zhou, *BioResources*, 2015, **10**, 2809-2822.
12. Y. Beeran, V. Bobnar, S. Gorgieva, Y. Grohens, M. Finšgar, S. Thomas and V. Kokol, *Rsc Advances*, 2016, **6**, 49138-49149.
13. J. Duan, S. Gong, Y. Gao, X. Xie, L. Jiang, Q. J. A. a. m. Cheng and interfaces, 2016, **8**, 10545-10550.

14. N. Song, D. Jiao, P. Ding, S. Cui, S. Tang and L. Shi, *Journal of Materials Chemistry C* 2016, **4**, 305-314.
15. W. Yang, Z. Zhao, K. Wu, R. Huang, T. Liu, H. Jiang, F. Chen and Q. Fu, *Journal of Materials Chemistry C*, 2017, **5**, 3748-3756.
16. N. Song, D. Jiao, S. Cui, X. Hou, P. Ding and L. Shi, *ACS applied materials interfaces*, 2017, **9**, 2924-2932.
17. W. Yang, Y. Zhang, T. Liu, R. Huang, S. Chai, F. Chen, Q. J. A. S. C. Fu and Engineering, 2017, **5**, 9102-9113.
18. N. Song, S. Cui, D. Jiao, X. Hou, P. Ding and L. Shi, *Carbon*, 2017, **115**, 338-346.
19. F. Ren, W. Tan, Q. Duan, Y. Jin, L. Pei, P. Ren and D. Yan, *Carbohydrate polymers*, 2019, **209**, 310-319.
20. P. Liu, C. Zhu and A. P. Mathew, *Journal of hazardous materials*, 2019, **371**, 484-493.
21. L. Li, B. Zhou, G. Han, Y. Feng, C. He, F. Su, J. Ma, C. J. C. S. Liu and Technology, 2020, 108229.